Immunofluorescence detection with quantum dot bioconjugates for hepatoma *in vivo*

Xuefeng Yu*
Wuhan University
Key Laboratory of Acoustic and Photonic Materials
    and Devices of Ministry of Education
Department of Physics
Wuhan 430072 China

Liangdong Chen*
Wuhan University
Cancer Center of Wuhan University
Wuhan 430072 China

Kaiyang Li
Wuhan University
Key Laboratory of Acoustic and Photonic Materials
    and Devices of Ministry of Education
Department of Physics
Wuhan 430072 China

Yan Li
Wuhan University
Cancer Center of Wuhan University
    and
Department of Oncology
Zhongnan Hospital of Wuhan University
Wuhan 430071 China

Si Xiao
Xuan Luo
Wuhan University
Key Laboratory of Acoustic and Photonic Materials
    and Devices of Ministry of Education
Department of Physics
Wuhan 430072 China

Jia Liu
Wuhan University
College of Chemistry and Molecular Sciences
Wuhan 430072 China

Li Zhou
Yuliang Deng
Wuhan University
Key Laboratory of Acoustic and Photonic Materials
    and Devices of Ministry of Education
Department of Physics
Wuhan 430072 China

Daiwen Pang
Wuhan University
College of Chemistry and Molecular Sciences
Wuhan 430072 China

Ququan Wang
Wuhan University
Key Laboratory of Acoustic and Photonic Materials
    and Devices of Ministry of Education
Department of Physics
Wuhan 430072 China

Abstract. The use of highly specific and highly sensitive immunofluorescent probes is a promising approach for biomedical imaging in living tissue. We focus on immunofluorescence with quantum dot bioconjugates for hepatoma detection *in vivo*. We synthesized specific immunofluorescent probes by linking quantum dots to AFP (alpha-fetoprotein) antibody for specific binding AFP—an important marker for hepatocellular carcinoma cell lines. In *in vivo* studies, the characteristic quantum dot (QD) fluorescent property is exhibited by the QDs-Anti-AFP probes in tumor and they demonstrate active tumor targeting and spectroscopic hepatoma imaging with an integrated fluorescence imaging system. We investigate the inhomogeneous distribution of the QDs-Anti-AFP probes in tumor by using a site-by-site measurement method to test their ability for distribution studies of cancer cells. These results demonstrate the practicality of QD bioconjugates as attractive fluorescent probes for biomedical detection. © *2007 Society of Photo-Optical Instrumentation Engineers.* [DOI: 10.1117/1.2437744]

Keywords: fluorescence; quantum dots; hepatoma; immunofluorescence.

1 Introduction

Quantum dots (QDs) are a promising alternative to organic immunofluorescent probes for cancer detection.[1–9] Several characteristics distinguish QDs from commonly used fluorophores, such as broad absorption spectra, size- and composition-tunable, narrow fluorescence emission, and very high levels of brightness and photostability.[10–16]

For *in vivo* detection, clinical values of QDs as immunofluorescent probes require them to have high sensitivity and high specificity for cancer cells.[2] In one previous study, QDs were linked to immunoglobulin G (IgG) and streptavidin to label the breast cancer marker Her2 on the surface of fixed and live cancer cells, which showed that QD probes can be very effective in cellular imaging and offer substantial advan-

*These authors contributed equally to this work.
Address all correspondence to Ququan Wang, Wuhan University, Key Laboratory of Acoustic and Photonic Materials and Devices of Ministry of Education and Department of Physics,, Wuhan, 430072, China; Tel.: +86 27 68758445; Fax: +86 27 68752569; E-mail: qqwang@whu.edu.cn

tages over organic dyes.[17] In another study, QDs were first used as stable fluorescent tracers for nonspecific uptake studies and lymph node mapping in living animals.[1] In an important improvement, PEG-coated QDs were functionalized with antibodies to prostate-specific membrane antigen and were intravenously injected in mice for tumor targeting and imaging.[2] Most recently, self-illuminating quantum dot conjugates as new probes were first used in *in vivo* imaging.[6] However, there is no reported study of using immunofluorescent QD bioconjugates for *in vivo* hepatic cancer detection.

In this study, we aim to examine the sensitivity and specificity of the QD probes to hepatoma in mice and achieve attractive biomedical detection. We synthesized specific immunofluorescent probes by linking QDs to alpha-fetoprotein (AFP) antibody for specific recognition of AFP—an important marker for hepatocarcinoma cell line HCCLM6 (Ref. 18). *In vivo*, we achieved active tumor targeting and sensitive spectroscopic hepatoma imaging with an integrated fluorescence imaging system. We also investigated the inhomogeneous distribution of the QD probes in tumor by using a site-by-site measurement method to test their ability for distribution studies of cancer cells in tumor. These results demonstrate the potential of QD probes as attractive immunofluorescent probes for cancer detection.

2 Materials and Methods

2.1 Materials

Core-shell QDs (ZnS-capped CdSe, Ref. 15) were synthesized by College of Chemistry & Molecular Sciences, Wuhan University. Human hepatocellular carcinoma cell lines[18] (HCCLM6) were provided by Liver Cancer Institute of Fudan University. EDC (1-(3-Dimethyl-aminopropyl)-3-ethylcarbodiimide hydrochloride, >98%) and NHS (*N*-hydroxysuccinimide, >98%) were purchased from Acros-Organics. Mouse anti-human monoclonal AFP antibody and RPMI-1640 culture medium were purchased from Sigma.

2.2 QDs Bioconjugation and Animal Preparations

We used a 1.5-ml solution of high-quality oil-soluble core-shell QD590 to synthesize water-soluble QDs according to a developed procedure.[15] These activated dots modified with thioglycolic acid were dissolved in phosphate-buffered saline (PBS) (0.08 mol/l, pH 7.4) containing 50 mmol EDC and 5 mmol NHS. Then, the QDs were reacted with 20 μl mouse anti-human monoclonal AFP antibodies at room temperature in a shaking incubator for 2 to 4 h. The final QD bioconjugates were purified by centrifugation at 6000 g for 10 min, and the suspension was dialyzed for 8 to 12 h. The QDs-Anti-AFP thus afforded were stored in refrigerator at 4°C.

Using protocols approved by the Institutional Animal Care and Use Committee of Wuhan University, $\sim 10^6$ prepared HCCLM6 cells were injected into a 6- to 8-week-old nude mouse subcutaneously. Tumor growth was monitored daily until it reached the acceptable size (0.5 to 1 cm in diameter). Then, the synthesized QDs-Anti-AFP probes were injected into the tail vein at 0.4 nmol for active targeting (four times). The time interval between each injection was about 24 h. The mice were placed under anesthesia by injection of 3% Nem-

butal at a dosage of 45 mg/kg for *in vivo* studies.

Some other mice bearing tumors of similar sizes (0.5 to 1 cm in diameter) were prepared under the same protocols for histological examination. The same dose (0.4 nmol) of QDs and QDs-Anti-AFP were injected into different mice for passive and active targeting. After a 24-h probe circulation, the mice were killed and tumors and major organs were removed and frozen. Tissue collections were cryosectioned into sections (10 μm thick), fixed with acetone at 0°C, and examined with a confocal fluorescence microscope (Leica TCS-SP2-AOBS-MP, D-68165, Mannheim, Germany).

2.3 Fluorescence Detection and Imaging

The fluorescence imaging system is shown in Fig. 1(A). The pulsed laser was provided by a Ti:sapphire laser (Mira 900, Coherent). Samples were excited at the wavelength of 400 nm using an optical frequency-doubling system. The beam was focused on samples with a lens. The fluorescence over the entire emission range was collected by a liquid-nitrogen-cooled CCD-array spectrometer (ACTON, Spectra-pro 2500I) along with imaging acquisition and analysis software. The following samples were prepared for fluorescence detection: (1) QDs and QDs-Anti-AFP and (2) QDs-tagged tumor tissue and normal tissue in a nude mouse [Fig. 1(A)].

2.4 Site-by-Site Measurement for Distribution Analysis

We selected 2500 sampling sites covering a square area from the periphery to the central area in the tumor of a nude mouse, and each side of the square consists of 50 equidistant sites. An *X-Y* axis translation stage was designed to shift the QD-labeled mouse automatically [Fig. 1(A)]. When the fluorescence emission of one site was collected, the stage was shifted 0.1 mm along one axis to focus the laser on the next site. After 2500 continuous collections, all the recorded emission peak intensities were processed by software to form a contour map (Fig. 2) to indicate the fluorescence intensity distribution of the detected area.

3 Results and Discussion

3.1 Spectral Characteristic

The QDs and the QDs-Anti-AFP probes have the same narrow and symmetric emission spectrums (Fig. 3). The corresponding emission peaks are at 590 nm and half-maximum values are only 20 nm. The QDs-Anti-AFP probes used in this study exhibit the same excellent spectral property as the original QDs. Note that the exposure times of QDs (8 ms) and QDs-Anti-AFP (10 ms) were different for spectral matching.

3.2 In vivo Cancer Detection

To investigate the specific binding of QDs-Anti-AFP to hepatoma *in vivo*, we used QDs-Anti-AFP to target AFP for active targeting.[2,19] AFP is the main component of mammalian fetal serum, which is synthesized by visceral endoderm of yolk sac and by fetal liver cells. The alteration of AFP blood level is an important marker for hepatocellular carcinoma, so that the accumulation and retention of AFP at the site of tumor
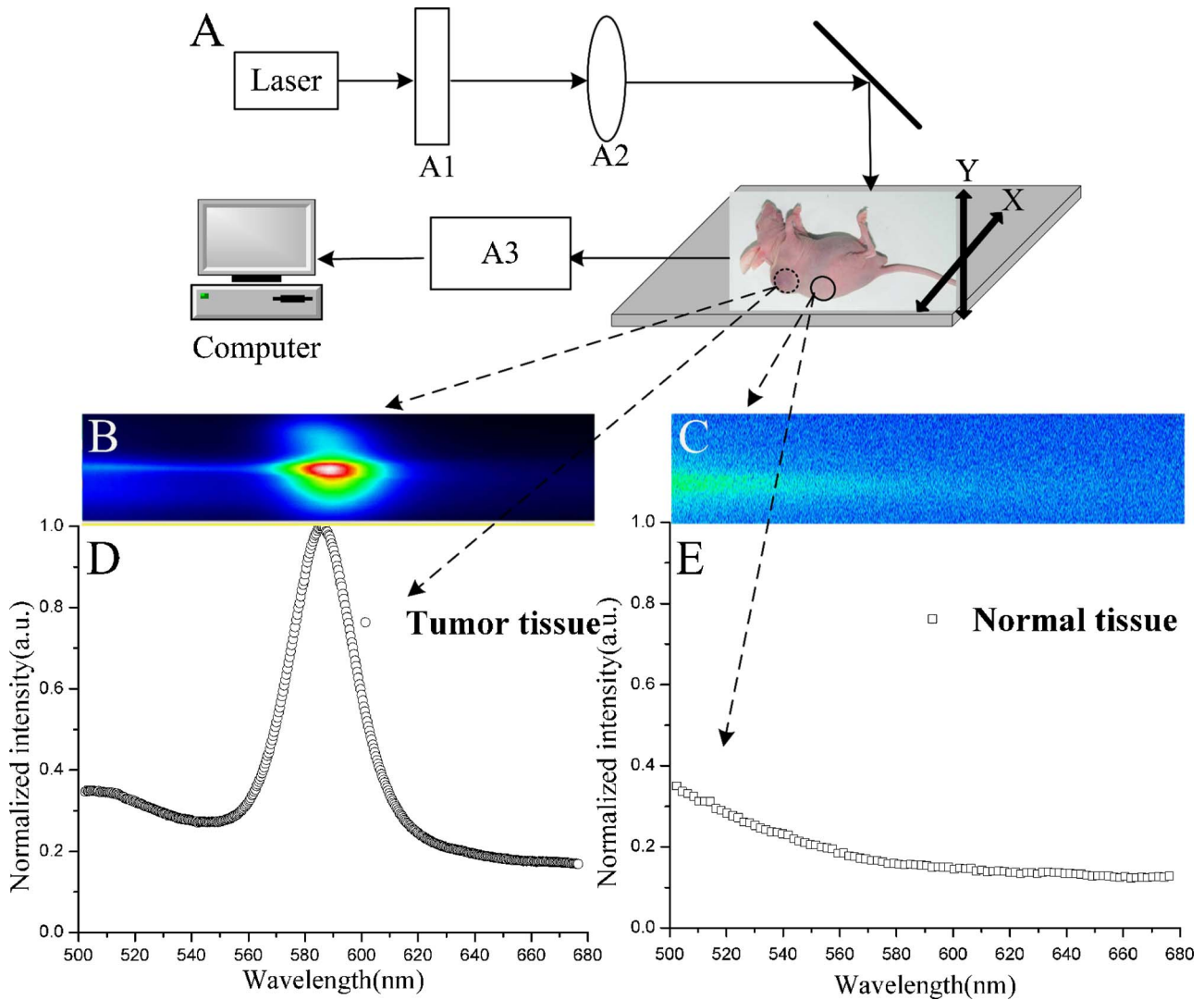
Fig. 1 (A) Simple optical layout of fluorescence imaging system: A1, optical frequency double system; A2, lens; A3, liquid-nitrogen cooled CCD-array spectrophotometer. (B) and (C) Spectroscopic imaging of (B) QDs-tagged tumor tissue and (C) normal tissue. (D) and (E) Emission spectrum of (D) QDs-tagged tumor tissue and (E) normal tissue. All the images and the spectrums were captured from a nude mouse with the same exposure time.

is the basis of immunofluorescence detection and targeted therapy for hepatic cancer.[20]

The fluorescence spectral feature of QDs-tagged tumor tissue almost fits that of the original QDs, and the quantitative spectral comparison [Figs. 1(D) and 1(E)] demonstrate that QD emission in tumor can be clearly distinguished from tissue autofluorescence. The spectroscopic imaging of the tumor tissue [Fig. 1(B)] exhibits strong QD fluorescence at 590 nm and relatively weak tissue autofluorescence. In contrast, the spectroscopic imaging of the normal tissue [Fig. 1(C)] shows only autofluorescence background. These results indicate that the QDs-Anti-AFP probes have specific and attractive binding to hepatoma *in vivo*. Note that the QD probes in nude mice were excited with femtosecond laser pulses in our study, so that the sampling sites for spectroscopic imaging are only a part of the tumor, not the whole mouse. The use of a macro-illumination system[1,2,21] should be an adapted alternative for whole animal studies.

In addition, the control study results with the same dose of nontargeted QDs and QDs-Anti-AFP are shown in Fig. 4 (0.4 nmol injected plus a 24-h latent period of probe circulation). Little QD accumulation was found in tumors due to passive tumor targeting, while QDs-Anti-AFP were detected by their clear characteristic fluorescence. Note that nonspecific liver and spleen uptake was apparent in organ uptake studies (image not shown), which is similar to that of QD-PSMA biconjucgates.[2]

3.3 Distribution Analysis

It has been shown that the QD probes can be targeted to tumor cells through both passive and active mechanisms (effected by cell membrane alignment along adhesive surfaces[19]), but passive targeting (due to permeation and retention of QDs at tumor sites[1,2,22,23]) is much less efficient than active targeting (Fig. 4) (due to QD-antibody binding to tumor-specific
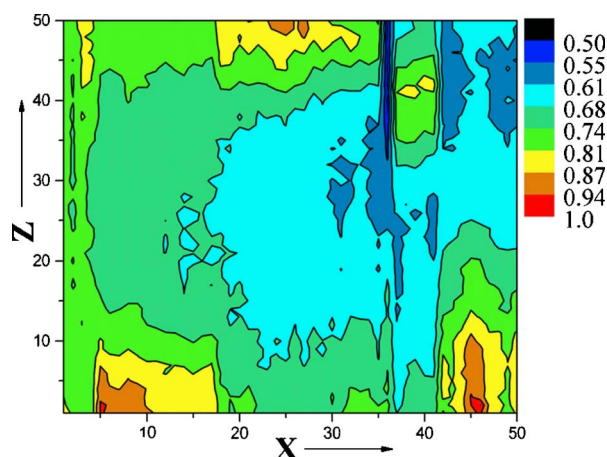
Fig. 2 Fluorescence intensity contour map of a detected cancerous area in the QDs-tagged tumor. Although all the sampling sites are in the tumor, their fluorescence intensities are different: cold colors represent lower fluorescence intensity in the area, while warm colors represent higher intensity. The detected cancerous area is from the periphery (corresponding to the lower left corner in the map) to the central area (corresponding to the upper right corner in the map) of the tumor. Thus, the map exhibits the inhomogeneous distribution of the fluorescence intensities in the detected area of the tumor.

antigens[2]). Thus, the necrotic cancer cells lacking specific antigen are almost deprived of the ability to bind to the QD probes, and the distribution of QD probes in tumor is mainly attributed to the density of cancer cells with specific antigens for active targeting. Consequently, a fluorescence intensity contour map (Fig. 2) was plotted by using the site-by-site measurement method already discussed for distribution analysis. Different colors in the map show the inhomogeneous distribution of cancer cells (with probes) in the detected area of the tumor. Since cold colors represent a lower fluorescence intensity in the area, and lower intensity corresponds to fewer QD probes among the sampling sites, it is clear that the cancer cells per field in the central area were less than the periphery area of the tumor. Although some singular points (such as the orange and red areas in the lower right-hand corner and the
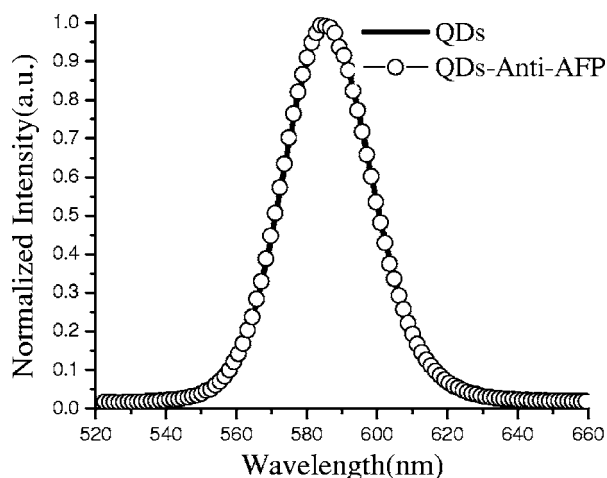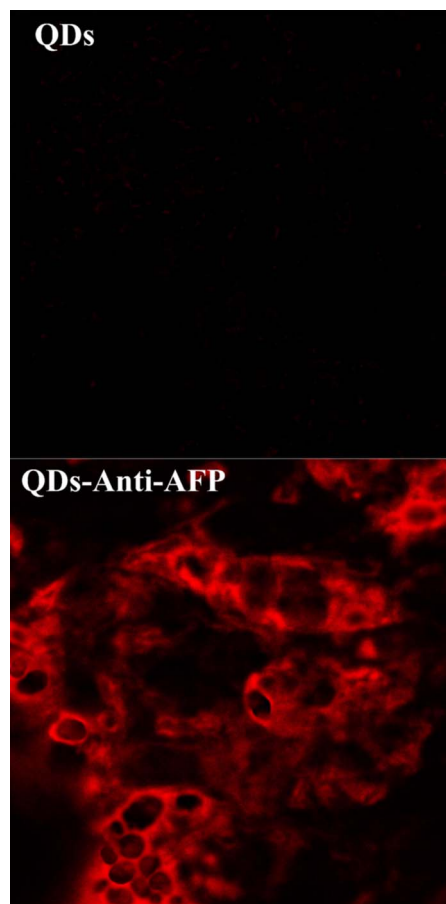

Fig. 4 Histological examination of QD passive and active targeting ability. The same dose of QDs and QDs-Anti-AFP (0.4 nmol and 24-h circulation) were injected in different mice bearing hepatoma of similar sizes (0.5 to 1 cm in diameter). The images were obtained from 10-μm thin tissue sections on a fluorescence microscope. Little QD accumulation was found in tumors due to passive tumor targeting, while QDs-Anti-AFP were detected by their clear characteristic fluorescence.

upper middle region of the map) do not match the whole tendency of color changes because of the complexity of tumor's structure, the fluorescence intensity contour map exhibit that the number of cancer cells (with probes) per field is lower inside than those outside.

Note that the result does not provide an absolute intensity comparison among these sites because several factors (such as complexity of tumor's structure and optical density of sampling sites) are difficult to normalize or calibrate. Instead, it is just a qualitative fluorescence intensity comparison, demonstrating the distribution of the cancer cells with QD probes in the tumor. Similarly, histological examinations have shown that the density of the vascular distribution in tumor is also inhomogeneous. It accumulates in the periphery and is scarce or absent in the central area, so that the process of nutrient competition causes more necrotic cells inside than outside in the tumor.[24] Further, the distribution result is consistent with the universal dynamics theory of tumor growth.[25] Unfortunately, the maximum shifting distance of the automatic X-Y axis translation stage in our study is only 5 mm, not enough for whole tumor studies. However, this problem could be

Fig. 3 Fluorescence spectral comparison between QDs and QDs-Anti-AFP.

solved with improved experimental conditions. Notwithstanding this limitation, these results demonstrate the QD probes are specific and sensitive enough for distribution analysis of a tumor *in vivo*.

4 Conclusions

Using QD bioconjugates as immunofluorescent probes for cancer detection is challenging. The indirect immunofluorescence method we adopt is based on the combination of AFP antibody and core-shell QD590. The synthesized QDs-Anti-AFP probes serve as secondary antibodies to combine with specific AFP (as primary antibody). The method we adopted is more convenient and practical than traditional streptavidin-biotin technique.[26] The optical examinations aim to archive specific and sensitive fluorescence detection with the complex QD probes. In *in vivo* conditions, the QDs-Anti-AFP in a tumor exhibit the characteristic QD fluorescence, and enable active tumor targeting and spectroscopic hepatoma imaging. In contrast, the same doses of nontargeted QDs were found to have little accumulation in tumors due to passive targeting following the same length of circulation. Further, by using the site-by-site measurement method, the probes show the practicality of the investigation of cancer cell distribution *in vivo* in a tumor. In addition, a remaining issue is the toxicity and metabolism of QD bioconjugates *in vivo*, which have been discussed by other groups.[2,27–30] We expect that the bright, specific, and sensitive QD-based bioconjugates will be ideal immunofluorescent probes for multiplexed cancer detection and diagnosis.

Acknowledgments

References

1. S. Kim, Y. T. Lim, E. G. Soltesz, A. M. De Grand, J. Lee, A. Nakayama, J. A. Parker, T. Mihaljevic, R. G. Laurence, D. M. Dor, L. H. Cohn, M. G. Bawendi, and J. V. Frangioni, "Near-infrared fluorescent type II quantum dots for sentinel lymph node mapping," *Nat. Biotechnol.* **22**, 93–97 (2004).
2. X. Gao, Y. Cui, R. M. Levenson, L. W. Chung, and S. Nie, "*In vivo* cancer targeting and imaging with semiconductor quantum dots," *Nat. Biotechnol.* **22**, 969–976 (2004).
3. I. L. Medintz, H. T. Uyeda, E. R. Goldman, and H. Mattoussi, "Quantum dot bioconjugates for imaging, labelling and sensing," *Nat. Mater.* **4**, 435–446 (2005).
4. X. Michalet, F. F. Pinaud, L. A. Bentolila, J. M. Tsay, S. Doose, J. J. Li, G. Sundaresan, A. M. Wu, S. S. Gambhir, and S. Weiss, "Quantum dots for live cells, *in vivo* imaging, and diagnostics," *Science* **307**, 538–544 (2005).
5. J. K. Jaiswal and S. M. Simon, "Potentials and pitfalls of fluorescent quantum dots for biological imaging," *Trends Cell Biol.* **14**, 497–504 (2004).
6. C. X. Min-Kyung So, A. M. Loening, S. S. Gambhir, J. Rao, "Self-illuminating quantum dot conjugates for *in vivo* imaging," *Nat. Biotechnol. Biol.* **24**, 339–343 (2006).
7. N. Y. Morgan, S. English, W. Chen, V. Chernomordik, A. Russo, P. D. Smith, and A. Gandjbakhche, "Real time *in vivo* non-invasive optical imaging using near-infrared fluorescent quantum dots," *Acad. Radiol.* **12**, 313–323 (2005).
8. T. P. Thomas, M. T. Myaing, J. Y. Ye, K. Candido, A. Kotlyar, J. Beals, P. Cao, B. Keszler, A. K. Patri, T. B. Norris, and J. R. Baker, Jr., "Detection and analysis of tumor fluorescence using a two-photon optical fiber probe," *Biophys. J.* **86**, 3959–3965 (2004).
9. J. K. Jaiswal, H. Mattoussi, J. M. Mauro, and S. M. Simon, "Long-term multiple color imaging of live cells using quantum dot bioconjugates," *Nat. Biotechnol.* **21**, 47–51 (2003).
10. W. C. Chan and S. Nie, "Quantum dot bioconjugates for ultrasensitive nonisotopic detection," *Science* **281**, 2016–2018 (1998).
11. M. Bruchez, Jr., M. Moronne, P. Gin, S. Weiss, and A. P. Alivisatos, "Semiconductor nanocrystals as fluorescent biological labels," *Science* **281**, 2013–2016 (1998).
12. C. M. Niemeyer, "Nanoparticles, proteins, and nucleic acids: biotechnology meets materials science," *Angew. Chem., Int. Ed.* **40**, 4128–4158 (2001).
13. X. Gao, W. C. Chan, and S. Nie, "Quantum-dot nanocrystals for ultrasensitive biological labeling and multicolor optical encoding," *J. Biomed. Opt.* **7**, 532–537 (2002).
14. A. P. Alivisatos, "Semiconductor clusters, nanocrystals, and quantum dots," *Science* **271**, 933–937 (1996).
15. H. Y. Xie and D. W. Pang, "Preparation of II–VI quantum dots and their application in biodetection," *Chinese J. Anal. Chem.* **32**, 1099–1103 (2004).
16. J. L. Swift, R. Heuff, and D. T. Cramb, "A two-photon excitation fluorescence cross-correlation assay for a model ligand-receptor binding system using quantum dots," *Biophys. J.* **90**, 1396–1410 (2006).
17. X. Wu, H. Liu, J. Liu, K. N. Haley, J. A. Treadway, J. P. Larson, N. Ge, F. Peale, and M. P. Bruchez, "Immunofluorescent labeling of cancer marker Her2 and other cellular targets with semiconductor quantum dots," *Nat. Biotechnol.* **21**, 41–46 (2003).
18. Y. Li, B. Tian, J. Yang, L. Zhao, X. Wu, S-L. Ye, Y.-K. Liu, and Z.-Y. Tang, "Stepwise metastatic human hepatocellular carcinoma cell model system with multiple metastatic potentials established through consecutive *in vivo* selection and studies on metastatic characteristics," *J. Cancer Res. Clin. Oncol.* **130**, 460–468 (2004).
19. A. Pierres, P. Eymeric, E. Baloche, D. Touchard, A.-M. Benoliel, and P. Bongrand, "Cell membrane alignment along adhesive surfaces: contribution of active and passive cell processes," *Biophys. J.* **84**, 2058–2070 (2003).
20. G. I. Abelev and T. L. Eraiser, "Cellular aspect of a-fetoprotein re-expression in tumors," *Semin Cancer Biol.* **9**, 95–107 (1999).
21. M. K. So, C. Xu, A. M. Loening, S. S. Gambhir, and J. Rao, "Self-illuminating quantum dot conjugates for *in vivo* imaging," *Nat. Biotechnol.* **24**, 339–343 (2006).
22. R. Duncan, "The dawning era of polymer therapeutics," *Nat. Rev. Drug Discovery* **2**, 347–360 (2003).
23. R. K. Jain, "Delivery of molecular medicine to solid tumors: lessons from *in vivo* imaging of gene expression and function," *J. Controlled Release* **74**, 7–25 (2001).
24. M. Scalerandi, A. Romano, G. P. Pescarmona, P. P. Delsanto, and C. A. Condat, "Nutrient competition as a determinant for cancer growth," *Phys. Rev. E* **59**, 2206 (1999).
25. A. Bru, S. Albertos, J. Luis Subiza, J. L. Garcia-Asenjo, and I. Bru, "The universal dynamics of tumor growth," *Biophys. J.* **85**, 2948–2961 (2003).
26. G. E. Jaiswal, J. K. H. Mattoussi et al., "Use of quantum dots for live cell imaging," *Nat. Methods* **1**, 73–78 (2004).
27. L. Braydich-Stolle, S. Hussain, J. Schlager, and M. C. Hofmann, "*In vitro* cytotoxicity of nanoparticles in mammalian germ-line stem cells," *Toxicol. Sci.* **13**, 13 (2005).
28. A. M. Derfus, W. C. W. Chan, and S. N. Bhatia, "Probing the cytotoxicity of semiconductor quantum dots," *Nano Lett.* **4**, 11–18 (2004).
29. J. Lovric, H. S. Bazzi, Y. Cuie, G. R. Fortin, F. M. Winnik, and D. Maysinger, "Differences in subcellular distribution and toxicity of green and red emitting CdTe quantum dots," *J. Mol. Med.* **83**, 377–385 (2005).
30. D. M. Warshaw, G. G. Kennedy, S. S. Work, E. B. Krementsova, S. Beck, and K. M. Trybus, "Differential labeling of myosin V heads with quantum dots allows direct visualization of hand-over-hand processivity," *Biophys. J.* **88**, L30–32 (2005).